RJC

RASĀYAN ***J. Chem.***
Vol. 16 | No. 3 |1525-1533| July - September | 2023
ISSN: 0974-1496 | e-ISSN: 0976-0083 | CODEN: RJCABP
http://www.rasayanjournal.com
http://www.rasayanjournal.co.in

CALCINATION AND HYDROTHERMAL PROCESSING OF BOVINES BONES FOR CALCIUM PHOSPHATES EXTRACTION

M. A. Irfa'i[1,2] , A. Prihanto[3], S. Muryanto[4], R. Ismail[1], J. Jamari[1] and A. P. Bayuseno[1,✉]

[1]Department of Mechanical Engineering, Diponegoro University, Semarang, 50275 Indonesia
[2] Department of Mechanical Engineering, Universitas Negeri Surabaya, Surabaya, 60231 Indonesia
[3]Chemical Engineering Vocational Program, Catholic Polytechnic Mangun Wijaya, Semarang, 50133 Indonesia.
[4]Department of Chemical Engineering, UNTAG University in Semarang, 50235 Indonesia
[1]Department of Mechanical Engineering, Diponegoro University, Semarang, 50275 Indonesia
✉Corresponding Author: apbayuseno@gmail.com

ABSTRACT

Bovine bone is a natural resource having valuable calcium phosphate compounds as a potential bioceramics powder feedstock. This study manipulated the calcium phosphates *via* hydrothermal processes after calcium phosphate-containing bone was calcined and extracted. Here the resulting powder precursors obtained after calcining at 900 °C for 5 hours were hydrothermally processed for varying times at 110°C (1–5 h), yielding mainly biphasic calcium phosphates (β-tricalcium phosphate and hydroxyapatite) formation with a minute lime according to XRD analysis. Calcination and hydrothermal processing can effectively produce a high amount of hydroxyapatite proportion (> 99 wt.%) with nano crystallite sizes (30-50 nm). After 5-hour calcination, the SEM images revealed the powder product with size uniformity (1 μm) and plate-like morphology. The powdered bovine bone was then subjected to DTA, DTG, and TG analyses to determine its thermal behavior. Calcination temperatures from 300 to 600 ^{O}C removed organic compounds and other impurities from powder matrices. Instead, the calcination of bovine bone at temperatures from 800 to 1000 ^{O}C supported the result of the stabilized microstructure of calcium-phosphate-bearing minerals, which would make valuable powder feedstock for hydrothermal synthesis. Results of the study demonstrated that simple calcination and subsequent hydrothermal processing of bovine bone providing major hydroxyapatite and minor β-tricalcium phosphate would get a depth insight into calcium phosphate resource recovery and recycling.

Keywords: Bovine Bone, Calcium Phosphates, Calcination, Hydrothermal Method, Hydroxyapatite, β-Tricalcium Phosphate

RASĀYAN *J. Chem.*, Vol. 16, No. 3, 2023

INTRODUCTION

Recently, much emphasis has been on generating new synthetic biomaterials from calcium phosphate (CaP) resources recovery of animal and biogenic wastes to fulfill the features of biomedical devices.[1] Biomaterials are similar to human tissue that can repair or replace bone because of their biocompatibility.[2] In this way, hydroxyapatite (HA) and β-tricalcium phosphate (β-TCP) are common biomaterials assisting in hard-tissue regeneration.[3,4] HA is also regarded as a non-toxic biomaterial with minerals similar to bone tissue.[5, 6] Human bone, in particular, contains the amount of HA bioceramic, accounting for roughly 70 % of the total.[7,8] Accordingly, there appears to be a growing demand for HA to repair bone defects.[9] Instead of HA material, β-TCP may donate Ca^{2+}, promoting higher osteoconductivity in a scaffold material.[10] Additionally, medical applications recognize HA coating on metallic body implants.[9,11-13] Further, HA can be extracted from eggshells,[14,15] cockles,[16] seashells,[17] oyster shells,[18,19,] and cuttlefish shells to provide a low-cost feedstock of calcium phosphate resources.[20,21] Calcium phosphate resources derived from biogenic materials are potential powder precursors for HA synthesis.[22] Animal bones,[21-24], and fish scales,[25] on the other hand, are potential bioceramics that provide calcium phosphates *via* calcination or hydrothermal synthesis of HA. Practically, animal bones and teeth contain 65 % inorganic nano-crystalline carbonate-

http://doi.org/10.31788/RJC.2023.1638427

hydroxyapatite solid rather than organic substances, with water accounting for the remaining 35% of the mass.[26] As a result, extracting calcium phosphate from natural bone yields a powder feedstock that is both cost-effective and beneficial to global sustainability.[27] Other methods for extracting calcium phosphate from natural bones include the subcritical water processes and alkaline hydrothermal hydrolysis.[21,28,29] In fact, nonstoichiometric and less crystalline apatite family crystals naturally form in animal bone, necessitating a subsequent aqueous crystallization strategy for growing and converting into crystalline hydroxyapatite (Ca/P ratio of 1.67), which can improve biocompatibility when used for bone regeneration.[4,26] In addition to the exact setting Ca/P ratio, the pH solution is a significant parameter for the aqueous crystallization of hydroxyapatite derived from bovine bone. Accordingly, crystallization, dissolution, and phase transformation processes of various calcium orthophosphates occurring under varying experimental conditions (pH and temperature) have become a concern in medical research.[30-32] Depending on the synthesis conditions, HA and β-TCP with the desired properties may be in some proportions forming from CP natural materials.[33] However, research on calcination and hydrothermally aqueous crystallization for synthesizing the biphasic calcium phosphates from natural sources of waste animal bones, and detailed mineral characterizations for validating the quality of the final powder products, is still limited. The present work examined the effectiveness of calcination and subsequent hydrothermal methods for extracting calcium phosphates from bovine bones. The current novelty and rationale related to an effective relationship between calcination reactions and hydrothermal processing for the recovery of calcium phosphate from bovine bones, which allows for the direct synthesis of major hydroxyapatite. This study also used X-ray diffraction (XRD), scanning electron microscopy (SEM/EDX), and Fourier transform infrared spectroscopy (FTIR) to characterize the structural properties of as-calcined and hydrothermally formed powder products. The calcination and hydrothermal processes can improve the purity and nanosize of the hydroxyapatite powder products while preserving particle morphology uniformity. This integrated powder processing method can add knowledge on recycling bovine bone into high-valued hydroxyapatite as biomedical materials.

EXPERIMENTAL

Material and Methods

The following process is to extract calcium phosphates, as shown in Fig.-1. Crushing and grinding raw bovine bone were performed to make the powder feedstock for this investigation. Moreover, the ground powder was heated in an oven at 900 ^{O}C for 5 hours. In an autoclave reactor, 2 g of the calcined powder was dissolved into distilled water with an S/L (solid/liquid) ratio of 1:3, in which an initial pH of 10 was set up by adding 6 mL of NaOH, and the autoclave was tightly closed and heated to 110 ^{O}C for 5 hours. At the end of hydrothermal synthesis, the precipitating solid was rinsed regularly with water and filtered through filter paper (Whatman@42) after separation before being desiccated in a 110 ^{O}C oven for 2 hours. SEM, FTIR, and XRD characterization analyses were on all powder products under examination.

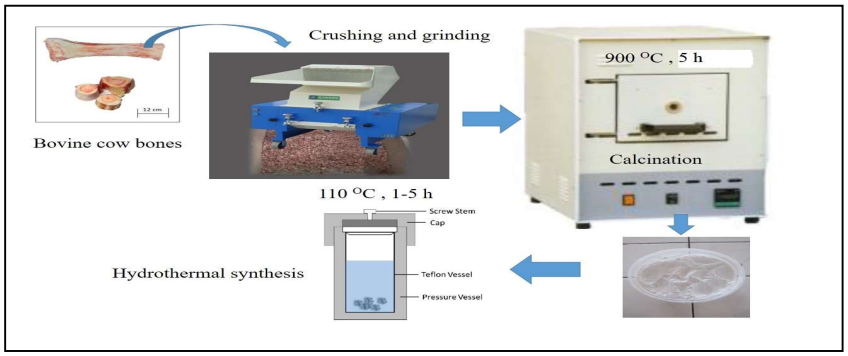

Fig.-1: Calcination and Hydrothermal Treatment of Bovine Cow Bones

Characterization

The powders were analyzed using XRD equipment (GE Sensing Technology, 30003 TT) set to the Bragg Brentano mode, a Cu-K (λ= 0.15406 nm), 40 kV, and 40 mA, as well as their parameters (5-90^{O} 2θ, 0.02^{O} steps, and 3s/step). The proposed phases were confirmed against the Crystallography Open Database (COD)

utilizing XRD Rietveld profile refinements (QualX PC-based match program) (Fulprof-2k, version 3.30). The COD's crystal structure model was also employed in the XRD Rietveld refinements.[34,35,36] As a result, the mass fractions of each crystalline phase generated by calcining and hydrothermal techniques totaled 100 wt. %.[37] Furthermore, the Williamson-Hall (W-H) formula was used to calculate the HA crystallite size, as shown in Equation (1), based on the preferred XRD patterns of HA contribution; where D_v is the crystal size in diameter; K is the shape factor as 0.9 for ceramic materials; λ is the wavelength of radiation in nanometers (λ= 0.15405 nm); and θ_{hkl} is the full-width half maximum (FWHM) for physical and instrumental broadening can both be related to peak broadening (Eq.-1).[38,39]

$$\beta_{hkl} \cos\theta_{hkl} = \frac{K\lambda}{D_v} + 4\varepsilon \sin\theta_{hkl} \quad (1)$$

This equation can be fitted to the standard straight-line equation (m = slope; c = intercept):

$$y = mx + c \quad (2)$$

In this study, Eq. 1 was used to estimate the preferred XRD peaks with significant intensities. The Williamson-Hall (W-H) plot calculates crystallite sizes based on the obtained line's intercept (Eq.-2). Instead, the morphology of the calcined and hydrothermally formed powders was analyzed using SEM/EDX method (Hitachi H-7100) at 20.0 kV and 1.00000 nA. Before SEM/EDX examination, the surface coating of the powder was with gold. This study also used FTIR (IR-Prestige 88) spectroscopy to characterize the structural properties of as-calcined bone and hydrothermally formed powders. This research can assist us in better understanding the phases associated with anions and substituting PO_4^{3-} and OH-groups. All spectra acquired were at a rate of 200 scans per second, with a spectral resolution of 2 cm^{-1} in bands ranging from 400 to 4000 cm^{-1}. Furthermore, TG-DTA on the calcined powder used thermal analysis (Perkin-Elmer TG-DTA-6300) for a fraction of the as-received bovine powder calcining in a muffle furnace at temperatures from 30 to 900 ºC for 10 ºC/min.

RESULTS AND DISCUSSION

The Properties of as-received and Calcined Powders

The elemental chemical compositions of as-received and calcined bovine powder samples obtained by XRF analysis are present in Table-1. The primary chemical elements of Ca and P are in the received and calcined samples at 900 ^{O}C for 5 hours, confirmed by the XRF analysis. Both bone powder samples appeared to correspond to biphasic calcium phosphate with a Ca/P ratio greater than 1.67. The Ca/P ratio increased after calcining the powder, resulting primarily in calcium phosphate minerals, which was later confirmed using an XRD Rietveld method.

Table-1: Chemical Elements in As-Received and Calcined Bovine Bones

Element	Mg	Al	Si	P	S	CL	K	Ca	Fe	Sr
As-received bone (wt.%)	0.15	0.04	0.32	5.33	0.15	0.08	0.08	16.3	0.05	0.01
Calcined bone (wt.%)	0.38	0.22	1.19	25.29	0.15	0.21	0.09	71.99	0.37	0.09

Figure-2 shows the XRD Rietveld refinement plot of the calcined powders samples. The phases generated in this powder were assigned crystallography Open Database (COD) # 9010050 (hydroxyapatite) and COD # 9005865 (β-tricalcium phosphate; β-TCP). The XRD spectra revealed an additional crystalline phase corresponding to CaO (COD # 900-6699). Increasing the calcination temperature to 900 ^{O}C promoted HA to convert into β-TCP and lime (CaO), as shown in Eq.-3.

$$Ca_{10}(PO_4)_6(OH)_2 \rightarrow 3Ca_3(PO_4)_2 + CaO + H_2O \quad (3)$$

Further quantitative XRD Rietveld analysis determined phase composition weight percentages and crystallite size of bovine bone hydroxyapatite (Table-2). In all tests, the primary phase of HA was discovered, with crystallite size variations ranging from 35 to 50 nm. Supposedly, calcination could facilitate the development of homogenous nanocrystalline HA. This discovery is similar to that of Chandrasekaran *et al.*[40]

Correspondingly, the HA- particles recovered from the calcined bovine powders are nanocrystalline. Figure-3 provides SEM images of calcined powder samples indicating the powder agglomeration. The

particle of agglomerated powder samples may relate to the numerous processes that happened during the drying of the precursor (Fig.-3). Agglomerated HA particles in calcined powder samples could be 1 m globules in size.

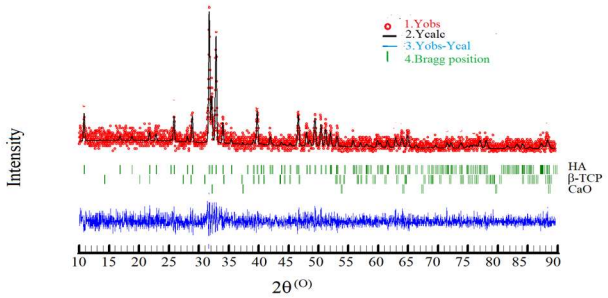

Fig.-2: XRD Rietveld Refinement Plots of Biphasic Calcium Phosphates (HA and -TCP) and Impurity Cao Generated by Calcining Bovine Bones for 5 h at 900 ^{O}C

Table-2: The Calcined Powders' Phase Compositions and Crystallite Size

Phases	Wt.%	Crystallite size (nm)
HA	99.1	36.5
TCP	0.7	
Lime	0.2	
Total	100	

The nanocrystalline HA appears to be generated by calcining and then merging particles of any shape. The findings of EDX microanalysis on the surface of calcined powders are also in Fig.-3, which revealed calcium and phosphorus spectra. Trace elements (Cu) are present in HA samples isolated from calcined bovine bones. The Ca and P ratio elemental spectra are evident, with predicted Ca/P values greater than HA stoichiometric values (1.67 to 1.5).[4] These findings suggested that Ca-containing minerals could form instead of hydroxyapatite.

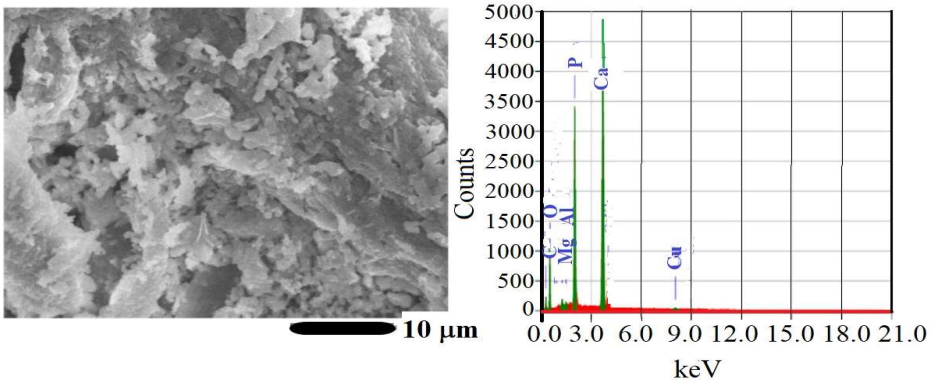

Fig.-3: SEM/EDX Examination of Calcined Bovine Bone Powder Samples

Hydrothermally Powdered Product Characteristics

The powder sample was hydrothermally synthesized at 110 ^{O}C for varying times (1-5 h), and results show no change in phase composition as the hydrothermal time increased (Fig.-4). Quantitative XRD Rietveld examination indicated that the dominant phase is still hydroxyapatite, with crystallite sizes ranging from 35 to 55 nm (Table-3). The hydrothermal approach used in this study appears to have had minimal influence on the modified crystallite sizes.

Further, a morphological study of the hydrothermally powdered product yielded SEM pictures of the tiny particles embedded in each agglomerated cluster, which match biphasic calcium phosphate particles (Fig.-5). Hydrothermal recrystallization of the dissolved calcium phosphate led to globule agglomerated morphology, as seen in Fig.-5. Based on the observed fracture surfaces of the particles, nanosized HA

particles appear to have been embedded in the aggregated formations during the hydrothermal process. By increasing the hydrothermal period to 5 h, all samples had almost homogenous spherule agglomerates (Fig.-5a-e). The particle size of the resulting hydrothermally powder appeared to have changed somewhat. However, particle size and crystallite size in HA powder samples did not match, showing that the particles collected are crystal agglomerates rather than single crystals.

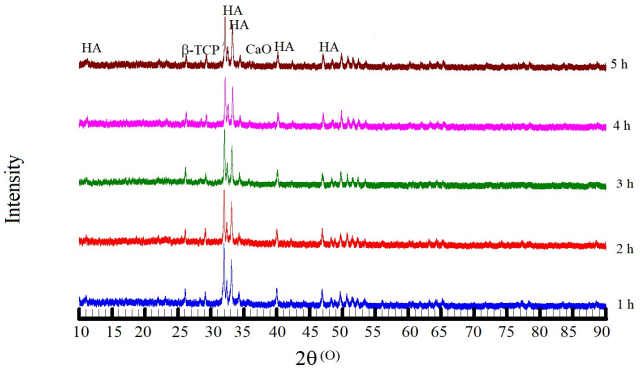

Fig.-4: XRD Powder Pattern Generated Hydrothermally at 110 ºC Over Time Intervals Varying from 1 to 5 h, with HA, β-TCP, and CaO Spectra Depicted

Table-3: Hydrothermally Produced Powder Phase Compositions and HA Crystallite Size at 110 ^{O}C for Varying Times

Phase (wt.%)	Time duration				
	1 h	2 h	3 h	4 h	5 h
HA	98.5	98.6	99.3	98.5	97.4
β-TCP	1.1	1.2	0.6	1.3	2.6
Lime	0.3	0.2	0.2	0.2	0.2
The crystallite size of HA (nm)	42.1	38.5	38.5	55.5	37.5

Furthermore, the morphology from the HA powder hydrothermally generated at 110 °C was the same as that of the as-calcined HA synthesized at 900 °C, with small particles suspended in a spherule agglomeration.

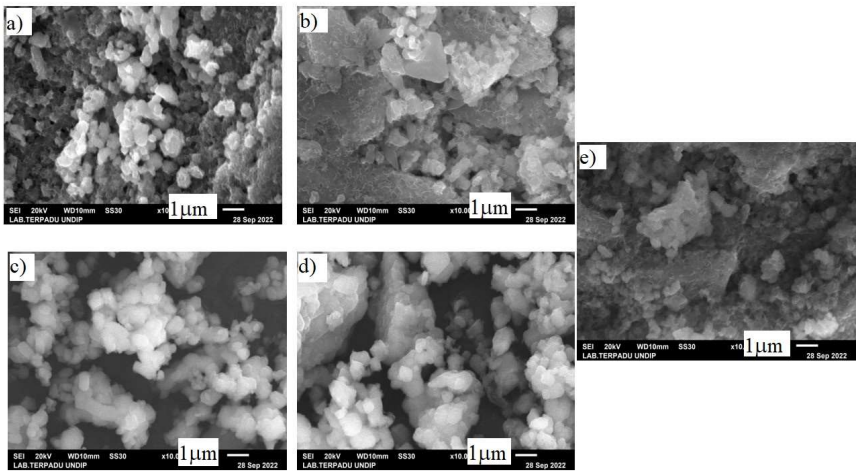

Fig.-5: SEM Images of Hydrothermally Generated Powders After; a) 1, b) 2, c) 3, d) 4, and e) 5 h at 110 ºC

FTIR spectroscopy results for hydrothermally produced powders at 110 ^{O}C for different periods are present in Fig.-6. The existence of the β-TCP phase correlated to PO_4 spectra, which are visible in all synthesized powders and accorded very well with the XRD result analysis. Also, the FTIR spectra of numerous hydrothermally powdered samples (Fig.-6) revealed the vibration modes of CO_3^{2-} group members at 1457 cm^{-1} and 1460 cm^{-1}, respectively. This substitution in the crystal lattice of HA is typical of precipitated

calcium phosphates, characterizing the production of carbonate-substituted B-type hydroxyapatite.[41] However, structured HA-CO_3^{2-} may be destroyed during calcination. The FTIR spectra of the calcined bovine powder (Fig.-6) reflected this observation.

Thermal Analysis

The thermal analysis determined the calcination and hydrothermal temperatures for extracting HA from raw bovine bone powder. Water removal resulted in a 12.6 % mass loss at 100 °C, according to the DTA/ DTG/ TG curves in Fig.-7.[42] At 630 °C, the temperature rose to 600 °C, resulting in an additional 41.9 % mass loss. This value reflected ammonium and water losses from surface powder, including water and carbonate removal from the crystal lattice.[43,44] After heating to 750 °C, there was a 1.7 % mass loss and a 1.1% mass loss after heating to 900 °C.

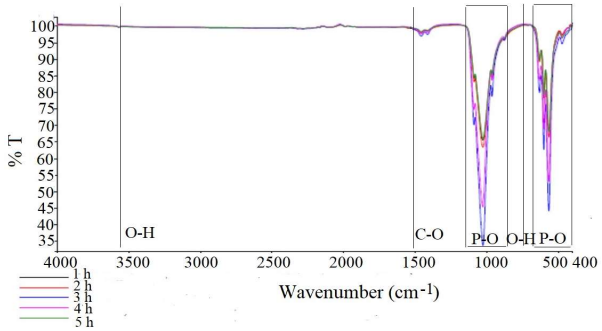

Fig.-6: FTIR Spectra of Hydrothermally Generated Powder at 110 °C Throughout 1 to 5 h

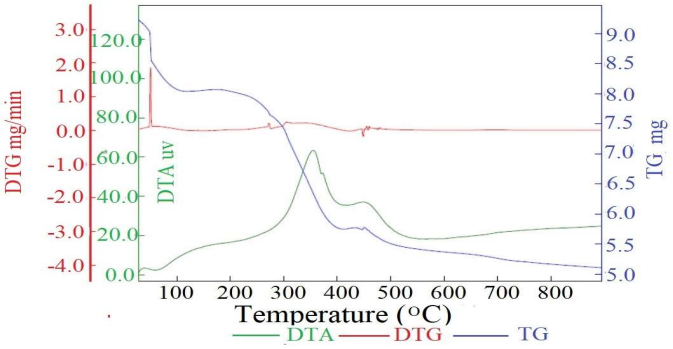

Fig.-7: DTA-DTG-TG Curves of Bovine Bones

Figure-7 also shows the variations in DTA in bovine bone powders. The data demonstrate an exothermic peak between 300 and 400 ^{O}C, resulting in a 30.25% loss in total weight mass. This sluggish loss continues up to 450 °C, leading to an additional 37.5% mass loss, followed by an extreme exothermic peak over 750 °C, resulting in a 54.4% mass loss. These initial peaks are related to hygroscopic water dehydration. The second peak could be the structured water loss during the crystalline transition. The temperature chosen for calcination and calcium phosphates (hydroxyapatite and β-TCP) remained steady when the exothermic peak reached its maximum at 900 ^{O}C. This DTA analysis result also validated the well-chosen calcination temperature employed in the current investigation. Other than those calcium phosphates, further hydrothermal processing at 110°C had no results.

CONCLUSION

Bovine bones, with their high calcium concentration, are promising bioceramics in synthesizing biphasic calcium phosphates, mainly hydroxyapatite. Calcination and subsequent hydrothermal processing of the ground bovine bone powder retrieved calcium phosphates with major hydroxyapatite (> 98 wt.%) and minor β-tricalcium phosphate. Using the Williamson-Hall (W-H) formula for calculating the crystallite size of hydroxyapatite validated nanosized particle agglomeration. As can be seen in the SEM micrograph, calcination, and hydrothermal processing resulted in spherule particle aggregation. The particles were

porous. As the calcination temperature increased, the particle size stayed constant, but the particles tended to be homogenous and spherical. As determined by SEM examination, the particle size of the synthetic powder (1 µm) is different from that of a crystallite measured by XRD analysis (40-50 nm). Similarly, additional hydrothermal processing of the calcined powder precursors had little effect on the morphology or crystallite size of the powder outputs. However, more research is required to create calcium phosphates as a scaffold material with a specified morphology by using chemical additives.

ACKNOWLEDGMENTS

We wish to thank the Head of the Mangunwijaya Catholic Polytechnic for allowing us to use the facilities in the Basic Chemistry Laboratory, as well as the Ministry of Higher Education Research for assisting with research *via* the Doctoral Dissertation Grant research scheme, contract number 345-36/UN7.6.1/PP/2022.

CONFLICT OF INTERESTS

The authors declare that there is no conflict of interest.

AUTHOR CONTRIBUTIONS

All the authors contributed significantly to this manuscript, participated in reviewing/editing, and approved the final draft for publication. The research profile of the authors can be verified from their ORCID ids, given below:

M.A. Irfa'i https://orcid.org/0000-0001-5343-1478
A. Prihanto https://orcid.org/0000-0003-2438-3977
S. Muryanto https://orcid.org/0000-0001-8330-9449
R. Ismail https://orcid.org/0000-0003-0445-3405
J. Jamari https://orcid.org/0000-0002-6172-2635
A. P. Bayuseno https://orcid.org/0000-0002-0882-4480

REFERENCES

1. A. Szcze, L. Ho and E. Chibowski, *Advances in Colloid and Interface Science*, **249**, 321(2017), https://doi.org/10.1016/j.cis.2017.04.007
2. N.I. Agbeboh, I.O. Oladele, O.O. Daramola, A.A. Adediran, O.O. Olasukanmi, and M.O. Tanimola, *Heliyon,* **6**, e03765(2020), https://doi.org/10.1016/j.heliyon.2020.e03765
3. F. Baino, S. Caddeo, G. Novajra and C. Vitale-Brovarone, *Journal of the European Ceramic Society,* **36(9)**, 2175(2016), https://doi.org/10.1016/j.jeurceramsoc.2016.01.011
4. S.V. Dorozhkin SV, *Acta Biomaterialia* 6(3), 715(2010), https://doi.org/10.1016/j.actbio.2009.10.031
5. S.U.D.Wani, S.P. Gautam, Z.L. Qadrie and H. Gangadharappa, *International Journal of Biological Macromolecules*, **163**, 2145(2020), https://doi.org/10.1016/j.ijbiomac.2020.09.057
6. P. Pawelzik, M. Carus, J. Hotchkiss, R. Narayan, S. Selke, M. Wellisch, M. Weiss, B. Wicke and M. Patel, *Resources, Conservation and Recycling,* **73**, 211(2013), https://doi.org/v10.1016/j.resconrec.2013.02.006
7. L. Ladu, and P. Morone, *Sustainable Product Consumers*, **28**, 911(2021).
8. T.V. Safronova, V.I. Putlyaev, M.A. Shekhirev, Y.D. Tretyakov, A.V. Kuznetsov and A.V. Belyakov, *Journal of the European Ceramic Society*, **29**, 1925(2009), https://doi.org/10.1016/j.jeurceramsoc.2008.12.012
9. M. Jamil, A. Elouahli, H. Khallok, B. El Ouatli and Z. Hatim, *Surfaces and Interfaces,* **17**, 100380(2019), https://doi.org/10.1016/j.surfin.2019.100380
10. B. Liu and D-X. Lun, *Orthopaedic Surgery,* **4**, 139(2012), https://doi.org/10.1111/j.1757-7861.2012.00189.x

11. G. Turnbull, J. Clarke, F. Picard, P. Riches, L. Jia, F. Han, B. Li and W. Shu, *Bioactive Materials* **3(3)**, 278(2018). https://doi.org/10.1016/j.bioactmat.2017.10.001
12. H. Khalid and A.A. Chaudhry, 2020, 4-Basics of hydroxyapatite-Structure, synthesis, properties, and clinical applications. In Handbook of Ionic Substituted Hydroxyapatites; Khan, A.S., Chaudhry, A.A., Eds, Woodhead Publishing: Sawston, UK: pp. 85-115.
13. L-H. Huang, X-Y. Sun and J-M. Ouyang, *Scientific Reports* **9**, 18979(2019), https://doi.org/10.1038/s41598-019-55428-9
14. G. Gergely, F. Weber, I. Lukacs, A.L. Toth, Z.E. Horvath, J. Mihaly and C. Balazsi, *Ceramic International,* **36(2)**, 803(2010), https://doi.org/10.1016/j.ceramint.2009.09.020
15. M. Akram, R. Ahmed and I. Shakir, W.A.W. Ibrahim and R. Hussain, *Journal of Materials Science,* **49**, 1461(2014), https://doi.org/10.1007/s10853-013-7864-x
16. X. Zhang and K.S. Vecchio, *Materials Science and Engineering C,* **26(8)**, 1445(2006), https://doi.org/10.1016/j.msec.2005.08.007
17. A. Singh and K.M. Purohit, *Journal of Bioprocessing & Biotechniques*, **1(2)**, 1(2011), https://doi.org/10.4172/2155-9821.1000104
18. J.H.G. Rocha, A. Lemos, F.S. Agathopoulos, P. Valério, S. Kannan, F.N. Oktar and J.M.F. Ferreira, *Bone* **37(6)**, 850(2005), https://doi.org/10.1016/j.bone.2005.06.018
19. S.C. Wua, H.C. Hsua, Y.N. Wuc and W.F. Hoc, *Materials Characterization*, **6(2)**, 1180(2011), https://doi.org/10.1016/j.matchar.2011.09.009
20. U. Ripamonti, J. Crooks, L. Khoali and L. Roden, *Biomaterials*, **30(7)**, 1428(2009), https://doi.org/10.1016/j.biomaterials.2008.10.065
21. N.A.M. Barakat, M.S. Khil, A.M. Omran, F.A. Sheikh and H.Y. Kim, *Journal of Materials Processing Technology*, **209(7)**, 3408(2009), https://doi.org/10.1016/j.jmatprotec.2008.07.040
22. J. Venkatesan and S.K. Kim, *Materials,* **3(10)**, 4761(2010), https://doi.org/10.3390/ma3104761
23. C.Y. Ooi, M. Hamdi and S. Ramesh, *Ceramic International*, **33(7)**, 1171(2007), https://doi.org/10.1016/j.ceramint.2006.04.001
24. A. Elkayar, Y. Elshazly and M. Assaad, *Bone and Tissue Regeneration Insights,* **2(7)**, 31(2009), https://doi.org/10.4137/BTRI.S3728
25. Y.C. Huang, P.C. Hsiao and H.J. Chai, *Ceramic International*, **37(6)**, 1825(2011), https://doi.org/10.1016/j.ceramint.2011.01.018
26. J.M. Sadowska, F. Wei, J. Guo, J. Guillem-Marti, Z. Lin, M-P Ginebra, and Y Xiao. *Acta Biomaterialia*, **96**, 605(2019), https://doi.org/10.1016/j.actbio.2019.06.057
27. L. Ladu and K. Blind, *Current Opinion in Green and Sustainable Chemistry*, **8**, 30(2017), https://doi.org/10.1016/j.cogsc.2017.09.002
28. A. Shavandi, AE-D. Bekhit, A. Ali and Z. Sun, *Materials Chemistry and Physics*, **149-150**, 607(2015), https://doi.org/10.1016/j.matchemphys.2014.11.016
29. A. Shavandi, V. Wilton and A.E-D. Bekhit, *Journal of the Taiwan Institute of Chemical Engineers*, **65**, 437(2016), https://doi.org/10.1016/j.jtice.2016.05.007
30. X. Guo, H. Yan, S. Zhao, L.Zhang, Y. Li and X. Liang, *Advanced Powder Technology*, **24**, 1034(2013), https://doi.org/10.1016/j.apt.2013.03.002
31. M. Sadat-Shojai, M-T. Khorasani, E. Dinpanah-Khoshdargi and A. Ahmad Jamshi, *Acta Biomaterialia*, **9**, 7591(2013), https://doi.org/10.1016/j.actbio.2013.04.012
32. N.A.S. Mohd Pu'ad, P. Koshy, H.Z. Abdullah, M.I. Idris and T.C. Lee, *Heliyon*, **5**, e01588(2019), https://doi.org/10.1016/j.heliyon.2019.e01588
33. M. Vallet-Regí and J.M. González-Calbet, *Progress in Solid State Chemistry*, **32**, 1(2004), https://doi.org/10.1016/j.progsolidstchem.2004.07.001
34. P.Y. Mahieux, J.E. Aubert, M. Cyr, M. Coutand and B. Husson, *Waste Management*, **30**, 378(2010), https://doi.org/10.1016/j.wasman.2009.10.023
35. R.S. Winburn, D.G. Grier, G.J. McCarthy and R.B. Peterson, *Powder Diffraction*, **15**, 163(2000), https://doi.org/10.1017/S0885715600011015

36. S. Grazulis, D. Chateigner, R.T. Downs, A.F.T. Yokochi, M. Quiros, L. Lutterotti, E. Manakova, J. Butkus, P. Moeck and A. Le Bail, *Journal of Applied Crystallography*, **42**, 1(2009), https://doi.org/10.1107/S0021889809016690
37. R.J. Hill and C.J. Howard, *Journal of Applied Crystallography*, **20**, 467(1987), https://doi.org/10.1107/S0021889887086199
38. G.K. Williamson and W.H. Hall, *Acta Metallurgica*, **1**, 22(1953), https://doi.org/10.1016/0001-6160(53)90006-6
39. M. Rabiei, A. Palevicius, A. Monshi, S. Nasiri, A. Vilkauskas and G. Janusas, *Nanomaterials*, **10(9),** 1627(2020), https://doi.org/10.3390/nano10091627
40. A. Chandrasekaran, S. Suresh and A. Dakshanamoorthy, *International Journal of Physical Sciences*, **8**, 1639(2013), https://doi.org/10.5897/IJPS2013.3990
41. D.L. Goloshchapov, V.M. Kashkarov, N.A. Rumyantseva, P.V. Seredinn, A.S. Lenshin, B.L. Agapov and E.P. Domashevskaya, *Ceramic International*, **39**, 4539(2013), https://doi.org/10.1016/j.ceramint.2012.11.050
42. W. Trisunaryanti, I. I. Falah, D. R. Prihandini and M. F. Marsuki, *Rasayan Journal of Chemistry*, **12(3)**, 1523(2019), https://doi.org/10.31788/RJC.2020.1315514
43. E. Garskaite, K-A. Gross, S-W. Yang, T.C-K. Yang, J-C. Yang and A. Kareiva, *CrystEngComm* **16(19)**, 3950(2014), https://doi.org/10.1039/c4ce00119b
44. K. Tõnsuaadu, M. Peld and V. Bender, *Journal of Thermal Analysis and Calorimetry*, **72**, 363(2003), https://doi.org/10.1023/A:1023917113850

[RJC-8427/2023]